Hindawi Publishing Corporation
Journal of Chemistry
Volume 2015, Article ID 964252, 10 pages
http://dx.doi.org/10.1155/2015/964252

Research Article

Spectra and Charge Transport of Polar Molecular Photoactive Layers Used for Solar Cells

Yuanzuo Li,[1] Dawei Qi,[1] Chaofan Sun,[1] and Meiyu Zhao[2]

[1]*College of Science, Northeast Forestry University, Harbin, Heilongjiang 150040, China*
[2]*Institute of Theoretical Simulation Chemistry, Academy of Fundamental and Interdisciplinary Sciences, Harbin Institute of Technology, Harbin, Heilongjiang 150080, China*

Correspondence should be addressed to Yuanzuo Li; yuanzuo.li@gmail.com and Dawei Qi; qidw98066@126.com

Received 1 April 2015; Revised 14 June 2015; Accepted 23 June 2015

Academic Editor: Luz Maria Rodriguez-Valdez

The ground state structures, HOMO and LUMO energy levels, band gaps $\Delta_{H\text{-}L}$, ionization potentials (IP), and electron affinities (EA) of three types of copolymer P1 and its derivatives P2, P3, and PBDT-BTA were investigated by using density functional theory (DFT) with B3LYP and 6-31G (d) basis set. On the base of optimized structures of ground states, their absorption spectra were obtained by using TD-DFT//Cam-B3LYP/6-31 G (d). Research shows that with the increasing conjugated units, HOMO energy levels increased, LUMO energy levels decreased, and band gaps decreased gradually. Moreover, their ionization potentials decreased and electron affinities increased along with the increase of conjugated chains, and absorption spectra red-shifted. In addition, the side chain has a significant effect on the properties of ground and excited states. In order to investigate the influence of conjugated units and side chain on the charge transport, their hole and electron reorganization energies were calculated, and the results indicated that Pb have a good hole transport capability. Considering the practical application, the HOMO and LUMO energy levels, band gaps, and absorption spectra under external electric field were studied, and the results proved that the external electric field has an effect on the optical and electronic properties.

1. Introduction

Electrically conducting polymers have been considered for numerous applications [1–4], such as organic thin-film transistors, conducting textiles, and solar cell. Donor-acceptor conjugated molecules are viewed as a kind of very attractive organic semiconductors because of their high chemical stability and uncommon versatility [5]. The semiconductors suitable as single component channel materials should facilitate the formation of an exciton through the cation and anion radicals, and they show both stable hole and electron transporting characteristics; on the other hand, the semiconductors are required to have a good match between their structures and metal electrodes to balance the charge injection barriers between the relative positions of HOMO and LUMO energy levels and the work function of electrodes.

For polymer solar cells (PSCs), donor-acceptor conjugated molecules as a p-type semiconductor should have good optical response and match of energy levels. For polymer solar cells, the photocurrent is generated after five process [6]: (1) the active layer absorbs photons to produce excitons; (2) excitons transfer to the donor-acceptor (D-A) interface; (3) excitons separate at the donor-acceptor interface and form free charges; (4) charges transport under an electric field; (5) charges are collected by electrodes. At present, much works have been done [7–18], and the photocurrent conversion efficiency (PCE) of polymer solar cells is still very low (reaching to about 10%) [7–10, 12, 16, 17]; how to improve its PCE is a key question for the purpose of realizing the commercialization and competing with traditional inorganic silicon photovoltaic cells. The main factors limiting the PCE of polymer solar cells have three points [11–13]: (1) the response range of active layer does not match with the solar spectrum; (2) the dissociation of excitons is difficult; (3) the carrier mobility of materials in current active layer seems very low compared with that of traditional inorganic silicon crystals. In order to improve the photocurrent conversion efficiency of polymer solar cells from the above aspects,

researchers have made great efforts. Mori et al. [14] fabricated low-band gap donor/acceptor polymer blend solar cells, presenting a short-circuit current density of 8.85 mA cm^{-2}, a fill factor of 0.55, an open circuit voltage of 0.84 V, and the high PCE of 4%, which demonstrates the potential of polymer/polymer blend solar cells as an alternative to polymer/fullerene solar cells. Klider and coworkers [15] synthesized the copolymer poly(2-methoxy-5-bromo-p-phenylenevinylen)/(2,5-dicyano-p-phenylenevinylene)(MB-PPV/DCN-PPV) using an electrochemical method, and the conclusions by cyclic voltammetry (CV), UV-Vis, and fluorescence (FL) spectroscopy showed that the conduction band is more stabilized in the copolymer than in homo polymer. Kim et al. [16] designed and synthesized a new poly{4,8-bis((2-ethylhexyl)thieno [3,2-b]thiophene)-benzo[1,2-b:4,5-b′]dithiophene-alt-2-ethylhexyl-4,6-dibromo-3-fluorothieno [3,4-b]thiophene-2-carboxylate} (PTTBDT-FTT) and an organic thin-film transistor showed high hole mobility of 2.1 $\times 10^{-2}$ $cm^2/(V{\cdot}s)$, and they also fabricated a single-junction bulk heterojunction photovoltaic cells, inverted photovoltaic cells, and a tandem photovoltaic device comprising PTTBDT-FTT, showing a maximum power conversion efficiency (PCE) of 7.44%, 7.71%, and 8.66%, respectively. In addition, researchers also have committed to design novel active layer materials with low-band gaps and high carrier mobility. Yu and coworkers [17] designed four new D-A copolymers, PCDT-BDPD (P1b), PDTC-BDPPD (P2b), PBDTTF-BDPD (P3b), and PBDTF-BDPD (P4b) based on diketopyrrolopyrrole (DPP) polymers, and the predicted PCEs of the new donor polymers reached up to about 10% in theory. Narayanana et al. [18] designed and synthesized a series of 3,4-ethylenedioxy thiophene (EDOT) and quinoxaline donor-acceptor (D-A) copolymers, P(EDOT-ACEQX), P(EDOT-BZQX), and P(EDOT-PHQX), exhibiting electrochemical band gap of 1.05, 1.0, and 0.99 eV, respectively.

In this work, density function theory (DFT) was used to study three types of copolymers [19]: a copolymer containing BDT and thiophene units in the main chain (no conjugated side-chain), and the copolymer is abbreviated as P1; introducing a conjugated side chain with no electron-withdrawing group into P1, which was named after P2; introducing a side chain with an electron-withdrawing group into P1, which was named after P3. Optical, electrochemical, and photovoltaic properties of P1, P2, and P3 were studied (see Figure 1); they are compared with those of a main chain type copolymer, PBDT-BTA, to get an insight into the effect of the introduction of conjugated side chain on photovoltaic properties of the conjugated copolymers.

2. Computational Methods

The molecular geometries of the several oligomers P1, P2, P3, and Pb (n = 1–3) were fully optimized using the DFT [20, 21] with B3LYP functional [22–24]. All calculations in this work were carried out using Gaussian 09 program package [25]. The 6-31G (d) basis set was used for all calculations. The HOMO, LUMO, and gap (HOMO-LUMO) energies were also deduced for the stable structures, and electron density corresponding to energy levels was studied. It is worth noting that DFT gives Kohn-Sham orbitals not molecular orbitals, which uses the KS orbitals to approximate the properties of the HOMO and LUMO. DFT combined with electron density analysis has been successful to investigate several series of polymers and charge transfer process under photon excitation [26–29]. Reorganization energies were obtained by means of calculation of the single point energy at the DFT//B3LYP level/6-31G(d), followed by the optimized geometries of different states (the neutral, cationic, and anionic geometries). Electronic transition energies and oscillator strengths of oligomers were obtained by using time dependent density functional theory (TD/DFT) [30], at the Cam-B3LYP/6-31G (d) level [31], which contains 65% long-range HF exchange.

3. Results and Discussion

3.1. Structural Properties. The ground state structures of P1, P2, P3, and Pb were optimized using DFT/B3LYP with 6-31G (d) basis set. The computing values (compromising the bond lengths and dihedral angles for their tripolymers) were listed in Table 1, and the number of atoms for the tripolymers structure of P1 and Pb were labeled in Supporting Materials (see Figure S1 in Supplementary Material available online at http://dx.doi.org/10.1155/2015/964252), and optimized cartesian coordinates and total energies were listed in Tables S1–S4. Compared to the bond length at same position of P1, P2, and P3, one can find the bond lengths for P3 that present the biggest values in the three molecules, and the value for P1 is the smallest. For C2-C3, the values for P1, P2, and P3 were 1.444, 1.446, and 1.447, respectively. It indicates that there is almost no change upon introducing a C=C and thiophene into the side chain of P1 and a cyan into the side chain of P2.

Moreover, it can be seen in Table 1 that the average dihedral angle of P3 is the biggest among P1, P2, and P3, indicating the conjugated main chain of P3 twisted seriously. For example, C1-C2-C3-S4, S4-C5-C6-C7, C8-C9-C10-S11, S11-C12- C13-C14, and C15-C16-C17-S18 for P3 are −15.1°, 36.7°, −7.6°, 35.7°, and −14.3°, respectively, and for P1 they are −3.9°, 3.9°, −7.5°, 7.7°, and −9.1°, respectively. So the structure of ground state for P1 tends to flatten among the three molecules. But, comparing P1 with Pb, the average dihedral angle of Pb seemed smaller than that of P1. One can make a conclusion that introducing a side chain can change the coplanarity at the micro level.

3.2. HOMO, LUMO, and Band Gaps ($\Delta_{H\text{-}L}$). The HOMO and LUMO energy levels and band gaps $\Delta_{\mathrm{H\text{-}L}}$ (difference between HOMO and LUMO) of the oligomers (n = 1, 2, 3) are computed, and the results are given in Table 2. Moreover, the energy levels and band gaps of the polymers are obtained by the extrapolation. As shown in Table 2, with the increasing conjugated units, HOMO energy levels increased slightly and LUMO energy levels decreased obviously, and the band gaps $\Delta_{\mathrm{H\text{-}L}}$ present a decreased tendency. Moreover, it can be seen in Figure 2 that with the increasing of conjugated main chain, the HOMO energy levels of the four molecules have a tiny change, but the LUMO energy levels of that change obviously,

Table 1: Selected optimized bond length and dihedral angles of P1, P2, P3, and PBDT-BTA (Pb) for unit $n = 3$.

	P1	P2	P3	Pb		
				Bond length (Å)		
C2-C3	1.444	1.446	1.447	C2-C3 (1.444)	C16-C17 (1.443)	C30-C31 (1.444)
C5-C6	1.443	1.450	1.451	C6-C7 (1.459)	C20-C21 (1.459)	C34-C35 (1.462)
C9-C10	1.443	1.446	1.446	C7-C8 (1.374)	C21-C22 (1.375)	C35-C36 (1.372)
C12-C13	1.444	1.449	1.450	C8-C9 (1.432)	C22-C23 (1.432)	C36-C37 (1.435)
C16-C17	1.448	1.447	1.448	C12-C13 (1.442)	C26-C27 (1.442)	
				Dihedral angles (°)		
C1-C2-C3-S4	−3.9	−10.7	−15.1	C1-C2-C3-S4 (−11.8)	C19-C20-C21-C22 (−9.4)	C35-C36-C37-C38 (1.9)
S4-C5-C6-C7	3.9	32.7	36.7	C5-C6-C7-C8 (12.1)	C21-C22-C23-C24 (−0.5)	
C8-C9-C10-S11	−7.5	−13.9	−7.6	C7-C8-C9-C10 (1.6)	C25-C26-C27-S28 (3.7)	
S11-C12-C13-C14	7.7	32.8	35.7	C11-C12-C13-S14 (1.3)	C29-C30-C31-S32 (−8.0)	
C15-C16-C17-S18	−9.1	10.2	−14.3	C15-C16-C17-S18 (−0.8)	C33-C34-C35-C36 (15.1)	

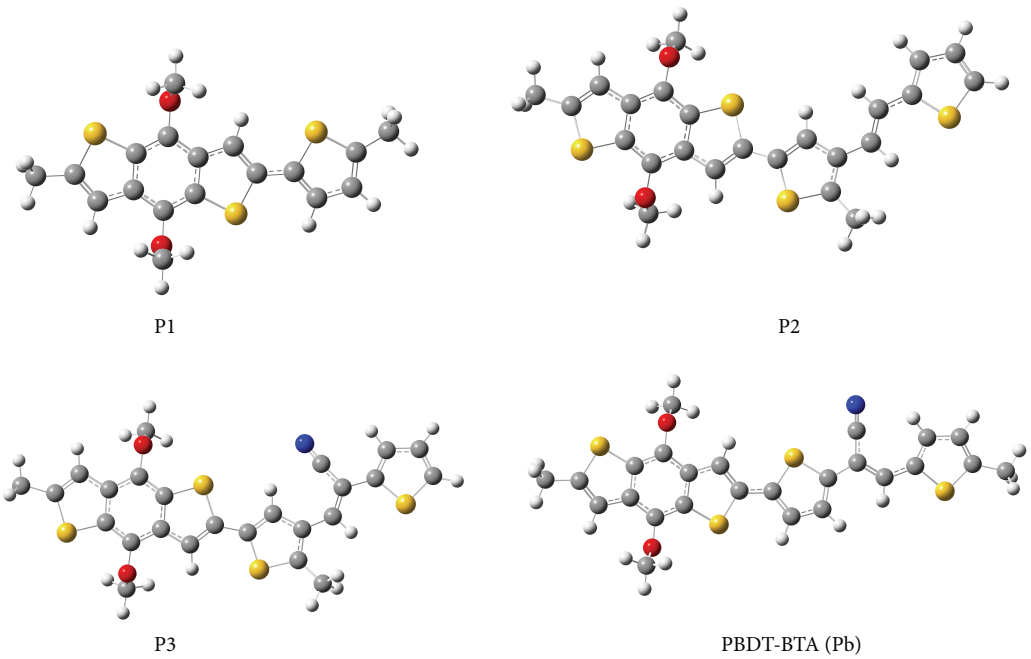

Figure 1: Chemical structures of P1, P2, P3, and PBDT-BTA (Pb).

while the band gaps have a good linear relationship with the reciprocal of conjugated unit n (see Figure S2).

Comparing P1 with P2, the HOMO and LUMO and band gaps for each of their conjugated unit ($n = 1, 2, 3$) have rough equal values (corresponding error of about 0.07 eV). But, contrasting the energy levels of P3 with P1, one can find that their LUMO energy levels have bigger differences than that of P1 and P2. In order to have a comprehensive investigation, one compared the energy levels of P3 with Pb and found that the LUMO energy levels of Pb are lower than that of P3. However, their HOMO energy levels also have a small difference. In a conclusion, the HOMO energy level of the four molecules is in this order: Pb > P3 > P2 > P1; their LUMO energy level is in this order Pb < P3 < P2 < P1. So their band gaps are in this order: Pb < P3 < P2 < P1, and change of energy gap results in bathochromic shifts in their absorption from Pb to P1.

Considering the fullerene-based heterojunction photovoltaic cells, copolymer as electron donor should have good energy match with fullerene (such as [60] PCBM). Usually, in theory, open voltage can be estimated through the following equation:

$$V_{oc} = \left(\frac{1}{e}\right)\left[\left|E_{HOMO}(D)\right| - \left|E_{LUMO}(A)\right|\right] - 0.3V, \quad (1)$$

where e means element electronic; $E_{HOMO}(D)$ and $E_{LUMO}(A)$ mean the donor HOMO energy and acceptor LUMO energy, respectively; 0.3 is the experience constants [32]. For P1–Pb as electron donor, $E_{HOMO}(D)$ energies are −4.79 eV, −4.74 eV, −4.99 eV, and −4.93, respectively; $E_{LUMO}(A)$ for [60] PCBM was obtained to be −3.09 eV at the DFT//B3LYP/6-31G(d). From (1), the difference between $E_{HOMO}(D)$ and $E_{LUMO}(A)$ with relatively large value has relatively higher open circuit voltage. It can be seen that the E_{HOMO} of P3 and Pb are

Table 2: Energy levels of HOMO and LUMO and energy gaps $\Delta_{H\text{-}L}$ of P1, P2, P3, and PBDT-BTA (Pb).

Molecules	Units	LUMO (eV)	HOMO (eV)	$\Delta_{H\text{-}L}$ (eV)
P1	$n = 1$	−1.47	−5.04	3.57
	$n = 2$	−2.07	−4.89	2.82
	$n = 3$	−2.28	−4.89	2.61
	$n = \infty$	−2.68	−4.79	2.11
P2	$n = 1$	−1.51	−5.00	3.49
	$n = 2$	−2.07	−4.86	2.79
	$n = 3$	−2.21	−4.83	2.62
	$n = \infty$	−2.58	−4.74	2.16
P3	$n = 1$	−2.10	−5.13	3.03
	$n = 2$	−2.39	−5.06	2.67
	$n = 3$	−2.53	−5.04	2.51
	$n = \infty$	−2.73	−4.99	2.26
Pb	$n = 1$	−2.39	−5.07	2.68
	$n = 2$	−2.74	−5.00	2.26
	$n = 3$	−2.87	−4.98	2.11
	$n = \infty$	−3.10	−4.93	1.83

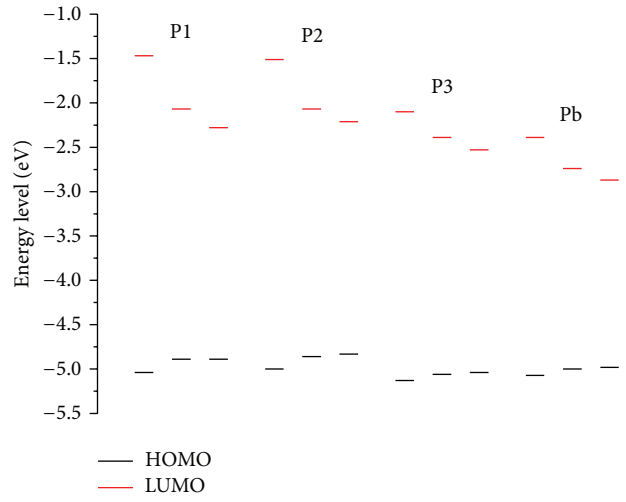

Figure 2: HOMO and LUMO energy levels of the oligomers (n = 1, 2, 3).

lower than that of P1 and P2 molecules, suggesting that the increased conjugated length can obtain relatively higher open circuit voltage.

Figure 3 shows HOMOs and LUMOs surface plots of the four tripolymer. From Figure 3, it can be seen that the electron densities of the HOMO of P1 are distributed on the whole main chain, and the electron densities of HOMO of P2, P3, and Pb are distributed on the left of the molecule. The electron densities of LUMO of the four molecules are distributed on the middle part of the main chain.

3.3. Ionization Potentials and Electron Affinities. Ionization potentials and electron affinities can predict the transport barrier of hole and electron in the organic solar cells [33, 34]. In order to explore the hole and electron transport,

Table 3: Ionization potentials and electron affinities of P1, P2, P3, and PBDT-BTA (Pb) (eV).

Units	P1		P2		P3		Pb	
	IP	EA	IP	EA	IP	EA	IP	EA
$n = 1$	6.17	0.30	6.01	0.50	6.15	0.92	6.04	1.35
$n = 2$	5.69	1.21	5.58	1.35	5.77	1.66	5.67	2.03
$n = 3$	5.62	1.57	5.47	1.61	5.72	1.93	5.54	2.29
$n \to \infty$	5.30	2.18	5.18	2.18	5.47	2.42	5.29	2.74

the ionization potentials (IP) and electron affinities (EA) of the four oligomers were calculated, and the results are listed in Table 3. As shown, with the increasing conjugated unit, IP decreased and EA increased. It indicates that the injection ability of hole and electron is improved with the increase of conjugated unit. Figure 4 shows the relationship between ionization potentials and electron affinities and the reciprocal of conjugated unit ($1/n$). It can be seen in Figure 4 that the IP and EA have a good linear relationship with the reciprocal of conjugated unit. Consequently, the IP and EA of the four polymers are obtained by the extrapolation. Table 3 shows that the IPs are 5.30 eV, 5.18 eV, 5.47 eV, and 5.29 eV for P1, P2, P3, and Pb, respectively, indicating that the injection capability of hole is in this order: P2 > Pb > P1 > P3. In addition, the values of EA are 2.18 eV, 2.18 eV, 2.42 eV, and 2.74 eV for P1, P2, P3, and Pb, respectively, and the injection capability of electron is in this order: Pb > P3 > P1 = P2.

3.4. Absorption Spectra. On the basis of optimized ground state structures, the absorption spectra of the four oligomers (n = 1, 2, 3) were investigated by TD-DFT//Cam-B3LYP/6-31G (d) method, and the results are listed in Table 4 and Tables S5–S8. It can be seen from Tables S5–S8 that, with the increasing conjugated units, the maximum absorption peaks of the four molecules have a red shift and the oscillator strengths increased except for P3. When n = 2, the oscillator strengths of P3 reached to the maximum 1.554 (1.169 and 1.264 for n = 1 and 3, resp.). From Table 4, it is found that the first excited state (S1) of the four tripolymers consists of the electron transition from HOMO to LUMO, and the corresponding absorption peaks are 2.815 eV (440.5 nm), 2.877 eV (430.9 nm), 2.21 eV (561.0 nm), and 2.409 eV (514.7 nm) for P1, P2, P3, and Pb, respectively. The site of absorption of four molecules shows that molecules P3 and Pb, with increasing conjugated length, display red-shifted absorption compared with the molecules P1 and P2.

Figure 5 shows the absorption spectra of P1, P2, P3, and Pb for n = 1 and n = 3. From Figure 5, one can see that with the increasing conjugated units, the maximum absorption peak of P3, have an obvious red shift about 5.68 eV (218.2 nm) and also the oscillator strength increases multiplied. Comparing with n = 1, the maximum absorption peak of other molecules (n = 3) red-shifted about 11.5 eV (107.8 nm), 13.22 eV (93.8 nm), and 11.96 eV (103.7 nm) for P1, P2, and Pb, respectively. Among them the absorption peak of P3 is the maximum and that of P2 is the minimum. Comparing the absorption spectra of P3 with the other three molecules, it can be found that P3 have a red shift and

Table 4: Transition energy and oscillator strengths for four molecules ($n = 3$).

Molecules	State	Transition energy (eV/nm)	Strength f	Contribution MO
P1	1	2.815/440.5	$f = 3.552$	H → L/0.61449
	2	3.255/380.9	$f = 0.020$	H-1 → L/0.45831
	3	3.595/344.9	$f = 0.464$	H-2 → L/0.49608
	4	3.745/331.1	$f = 0.038$	H-4 → L/0.44023
	5	3.816/324.9	$f = 0.040$	H-3 → L/0.36946
P2	1	2.877/430.9	$f = 2.856$	H → L/0.58998
	2	3.188/388.9	$f = 0.675$	H → L+1/0.46750
	3	3.601/344.4	$f = 1.096$	H-2 → L/0.30969
	4	3.701/335.1	$f = 0.559$	H-4 → L/0.34570
	5	3.728/332.6	$f = 0.148$	H-5 → L/0.46236
P3	1	2.210/561.0	$f = 1.264$	H → L/0.66110
	2	2.384/520.0	$f = 0.218$	H → L+1/0.61856
	3	2.442/507.8	$f = 0.275$	H-1 → L/0.58972
	4	2.565/483.4	$f = 0.249$	H-1 → L+1/0.52039
	5	2.638/469.9	$f = 0.008$	H → L+2/0.63202
Pb	1	2.409/514.7	$f = 6.003$	H → L/0.52475
	2	2.686/461.6	$f = 0.099$	H → L+1/0.47191
	3	3.030/409.2	$f = 0.583$	H-1 → L+2/0.29611
	4	3.283/377.7	$f = 0.030$	H-2 → L/0.33363
	5	3.406/364.0	$f = 0.127$	H-2 → L+1/0.35426

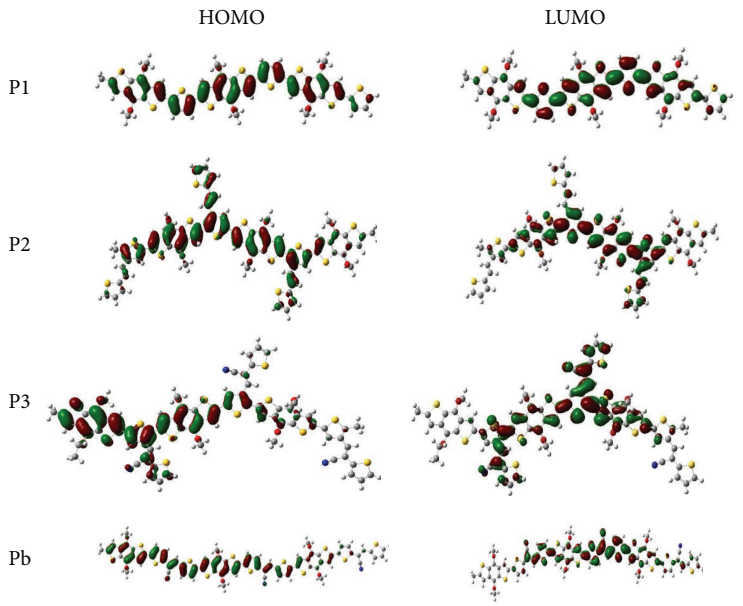

Figure 3: HOMOs and LUMOs surface plots of P1, P2, P3, and PBDT-BTA (Pb) ($n = 3$).

the values are 10.29 eV (120.5 nm), 9.53 eV (130.1 nm), and 26.78 eV (46.3) nm for P1, P2, and Pb, respectively. The second absorption peaks corresponding to the excited state (S2) have a similarity for the four molecules. It can be seen from Table 4 that all the second absorption peaks of P1, P2, P3, and Pb correspond to the excited state S3. Transition energy of S3 is 344.9 nm, 344.4 nm, 507.8 nm, and 409.2 nm and absorption strengths are 0.464, 1.096, 0.275, and 0.583, with composition of H-2 → L, H-2 → L, H-1 → L, and H-1 → L+2, respectively.

3.5. Reorganization Energies. The reorganization energy can be used to estimate the charge transfer characteristic in organic material. According to the Marcus theory [35, 36], the charge transfer rate can be expressed by the following formula [35]:

$$\kappa_{ET} = A \exp\left[\frac{-\lambda}{4\kappa_B T}\right], \quad (2)$$

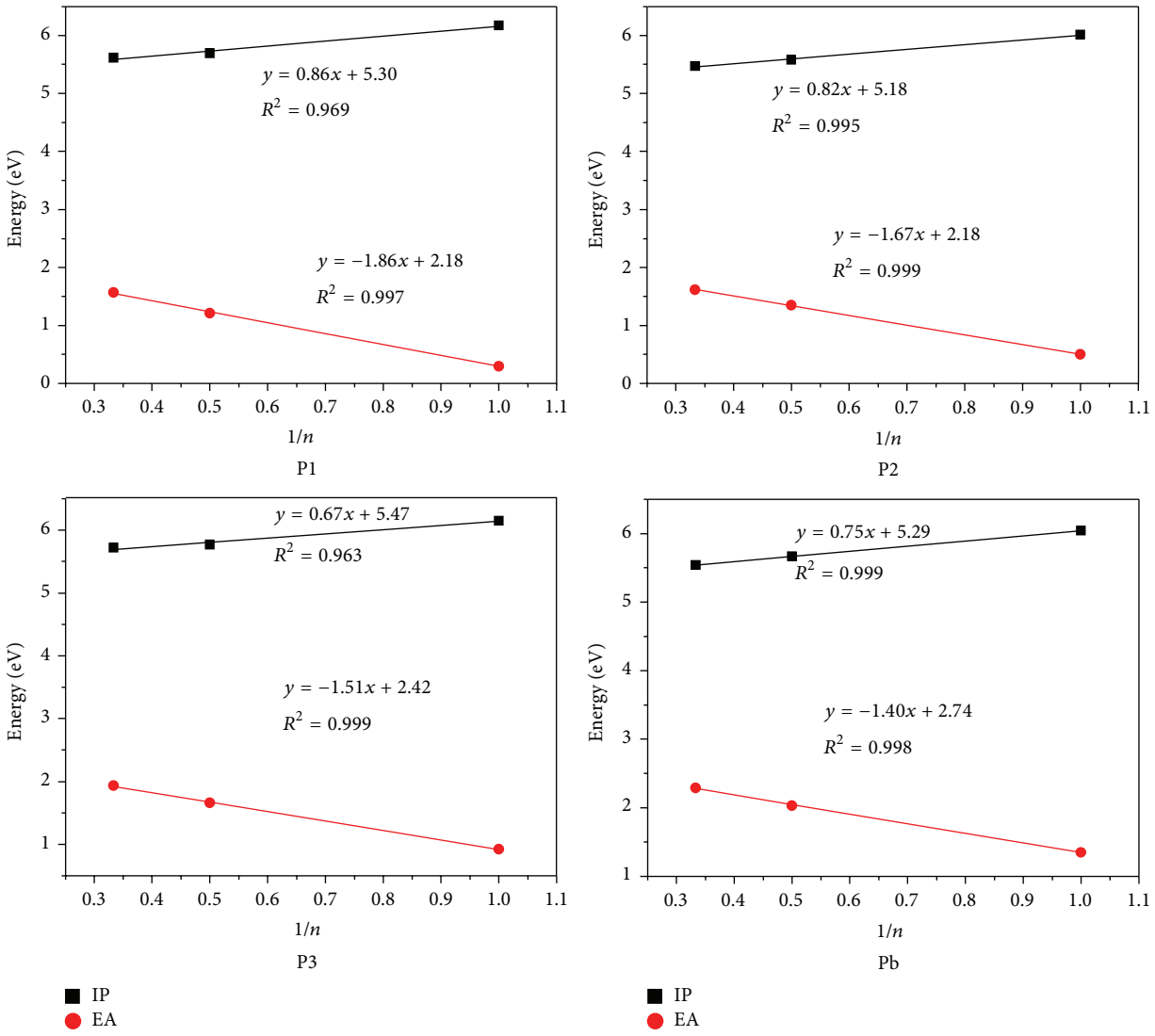

FIGURE 4: The relationship between ionization potentials (IP) and electron affinities (EA) of P1, P2, P3, and PBDT-BTA (Pb) and the reciprocal of conjugated unit ($1/n$).

where T is the temperature, κ_B is the Boltzmann constant, λ is reorganization energy, and A is electronic coupling. Among them, the reorganization energy is divided into two forms [37–40], one is the intermolecular reorganization energy and another is the intramolecular reorganization energy. However, the intermolecular reorganization energy has a tiny relationship with the charge transfer rate and has no significant effect on the electron transfer [39–41]. The intramolecular reorganization energies λ_h (which is defined as the reorganization energy of hole) and λ_e (which is defined as the reorganization energy of electron) can be expressed by the following formula:

$$\lambda_e = \left(E_0^- - E_-\right) + \left(E_-^0 - E_0\right)$$
$$\lambda_h = \left(E_0^+ - E_+\right) + \left(E_+^0 - E_0\right), \quad (3)$$

where E_0^+ (E_0^-) is energy of the cation (anion) calculated with the optimized structure of the neutral molecule; E_+ (E_-) is the energy of the cation (anion) calculated with the optimized cation (anion) structure; E_+^0 (E_-^0) is the energy of the neutral molecule calculated at the cationic (anionic) state; E_0 is the energy of the neutral molecule at the ground state. The calculated molecular reorganization energies of P1, P2, P3, and Pb were listed in Table 5. The results present various changes with the increase of conjugated units.

When the conjugated unit $n = 1$, hole reorganization energies are in this order: P2 < Pb < P3 < P1, in which P2 and Pb have a lower hole reorganization energies; electron reorganization energy is in this order: P2 < P3 < Pb < P1. But when $n = 2$, the electron reorganization energy of the four molecules is in this order: Pb < P1 < P2 ≈ P3, which have the same tendency with that of the tripolymers. In addition, the hole reorganization energy of the dipolymers is in this

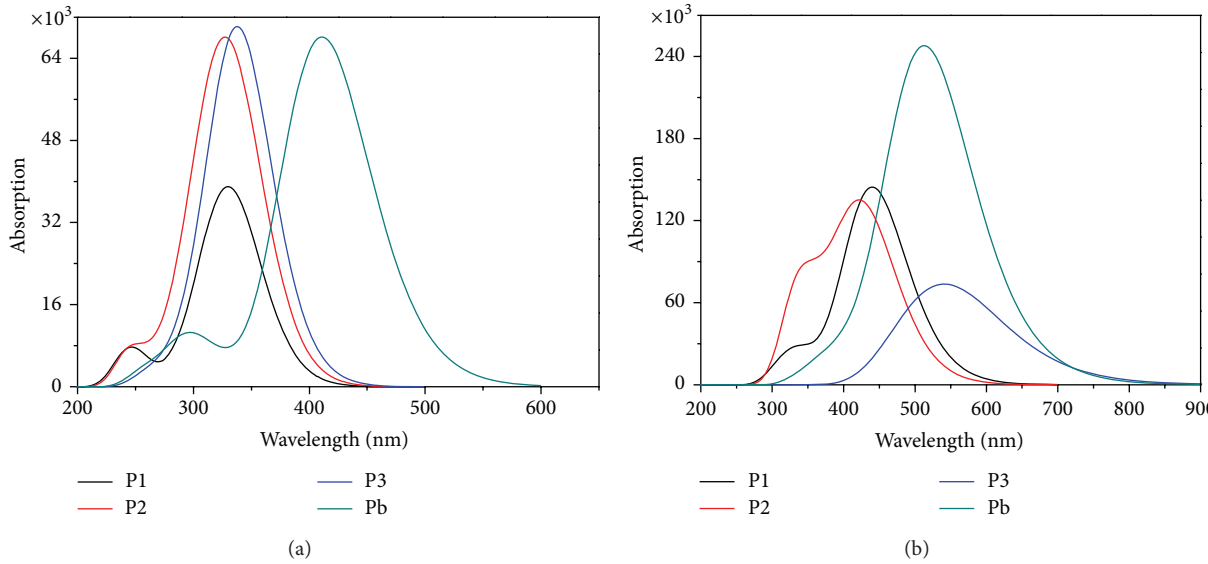

Figure 5: Absorption spectra of P1, P2, P3, and PBDT-BTA (Pb) for (a) $n = 1$ and (b) $n = 3$.

Table 5: Calculated molecular reorganization energies of four molecules ($\times 10^{-1}$ eV).

		P1	P2	P3	Pb
$n = 1$	λ_e	3.10	2.45	2.68	2.87
	λ_h	4.67	3.12	3.82	3.77
$n = 2$	λ_e	2.50	3.24	3.24	1.86
	λ_h	3.58	2.30	3.86	2.69
$n = 3$	λ_e	1.92	2.54	2.55	1.29
	λ_h	2.81	1.98	2.18	1.85

order: P2 < Pb < P1 < P3, which is different from that of the tripolymers: Pb < P2 < P3 < P1. In conclusion, Pb have a good hole transfer capability.

3.6. Field Effect on Optical Character. For solar cells, electric field originates from the p-n heterojunction [42]. In practical application, the active layer in the solar cell panel will be affected by the electric field produced by the system, resulting in the properties of changing spectra. The absorption peaks and oscillator strengths of P1, P2, P3, and Pb ($n = 1, 2$) under external electric field are listed in Table S9 and Table 6.

Along with the increasing electric field strengths ($F = 1\times10^{-3}$, 2×10^{-3}, and 3×10^{-3} a.u.), the transferred orientation of the charge is along the molecular skeleton. Table S9 shows that the change of the absorption peaks of monomers is not obvious, indicating that the external electron field has no significant effect on the optical properties of the monomers. When $n = 2$, the absorption spectra of all the molecules spectra have an evident red-shift with the increase of external electron field, and the red-shifted values are 38.6 nm, 34.8 nm, 115.9 nm, and 647.2 nm for P1, P2, P3, and Pb, respectively. Comparing the absorption spectra under $F = 3 \times 10^{-3}$ a.u., Pb has a remarkable red-shift (660.1 nm) and P3 presents a small red-shift (19.8 nm), indicating that when $n = 2$, the influence of external electron field on the optical property of Pb is interesting. But in the sake of the oscillator strength, the external electron field makes the absorption strength of Pb decrease maximally (from 3.536 to 0.066), which is bad for the performance of the organic solar cells.

Table 7 and Table S10 give the HOMO snd LUMO energy levels and band gaps of P1, P2, P3, and Pb ($n = 1, 2$) under external electric field. It can be seen in Table S10 that the external electron field still has no obvious effect on the energy levels and band gaps of the monomers, so we do not give over much attention to the monomers. Figure 6 gives the change of energy levels of the dipolymers with the increasing electron field and the specific results (see Table 7). From Figure 6, one can find that with the increase of electron field, HOMO increased and LUMO decreased obviously, in which the HOMO energy level is in this order: Pb > P2 ≈ P3 > P1; LUMO energy level is in this order: Pb < P3 < P2 < P1. Figure 7 shows the change tendency of band gaps with the increase of external electron field. As shown, it can be seen that the band gaps are decreased in different degrees with the increasing electron field, in which the band gaps of P3 changed obviously (1.56 eV), but the band gaps of Pb are the least corresponding to each of electron field strengths (1.57 eV, 0.58 eV, and 0.21 eV for $F = 1 \times 10^{-3}$, 2×10^{-3}, and 3×10^{-3} a.u., resp.), indicating that Pb have good photoelectric properties.

4. Conclusion

The properties of ground state and excited state of poly[(benzodithiophene- 2,6-diyl)(2,5-thienylene)] (P1) and its derivatives P2, P3, and PBDT-BTA (Pb) were investigated by using DFT//B3LYP/6-31G(d) and TD-DFT//Cam-B3LYP/6-31G(d) method, respectively. The results of energy levels and absorption spectra showed that with the increasing conjugated length, the site of absorption peak of molecules P3 and Pb displays the red-shifted absorption compared

Table 6: Absorption spectra and oscillator strengths of the dipolymers under external electric field.

Field ($\times 10^{-3}$ a.u.)	P1	P2	P3	Pb
1	415.1 (2.157)	414.3 (1.864)	423.5 (1.481)	501.1 (3.536)
2	427.8 (1.991)	425.5 (1.730)	438.3 (1.278)	576.9 (0.974)
3	453.7 (1.662)	449.1 (1.444)	539.4 (0.001)	1148.3 (0.066)

Table 7: HOMO and LUMO energy levels and band gaps of the dipolymers under external electric field (eV).

Field ($\times 10^{-3}$ a.u.)	P1			P2			P3			Pb		
	H	L	$\Delta_{H\text{-}L}$	H	L	$\Delta_{H\text{-}L}$	H	L	$\Delta_{H\text{-}L}$	H	L	$\Delta_{H\text{-}L}$
1	−4.83	−2.13	2.70	−4.76	−2.07	2.69	−4.82	−2.66	2.16	−4.65	−3.09	1.56
2	−4.62	−2.29	2.33	−4.50	−2.40	2.10	−4.50	−3.12	1.38	−4.20	−3.62	0.58
3	−4.38	−2.51	1.87	−4.19	−2.88	1.31	−4.16	−3.57	0.59	−4.04	−3.83	0.21

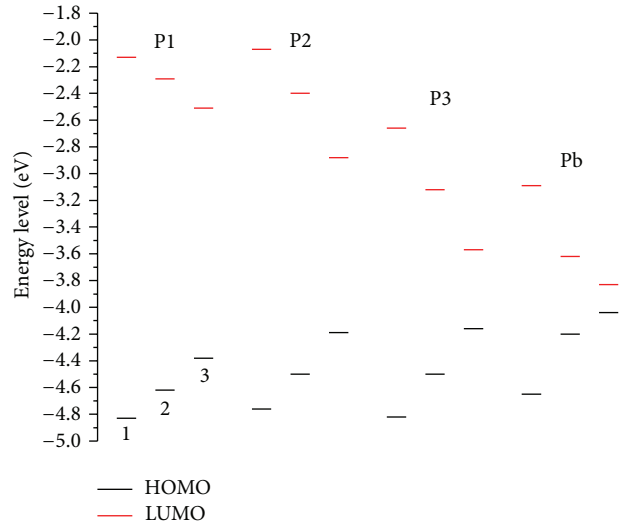

Figure 6: The changes of energy level of the dipolymers with the increasing electric field.

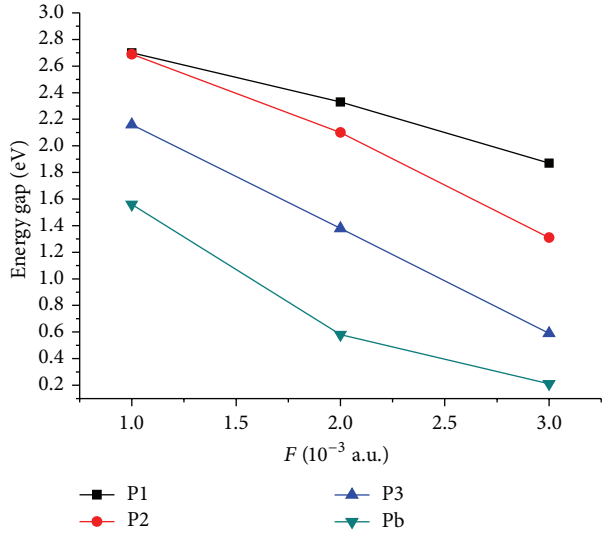

Figure 7: The changes of band gap of the dipolymers along with the increasing electric field.

with the molecules P1 and P2, and this trend is consistent with the change of band gaps. In addition, the effects of the external electric field on the optical and electronic properties were investigated, and it was found that energy level and absorption were changed by the changed external electric field. Evaluation of higher open circuit voltage suggested that the E_{HOMO} of P3 and Pb are lower than that of P1 and P2 molecules, meaning that the increased conjugated length can obtain relatively higher open circuit voltage. However, the result of charge transport parameters showed that among four molecules, the injection capability of hole of P2 is higher, and the injection capability of electron of Pb is higher. The hole transport ability of P3 and Pb is weaker than that of P2 from the calculation of reorganization energy. Therefore, it is important to simultaneously increase the optical absorption and improve the charge transport ability of [(benzodithiophene-2,6-diyl)(2,5-thienylene)] for further molecular design in the field of solar cells.

Conflict of Interests

The authors declare that there is no conflict of interests regarding the publication of this paper.

Acknowledgments

This work was supported by the Fundamental Research Funds for the Central Universities (Grant no. 2572014CB31), the Heilongjiang Provincial Youth Science Foundation (Grant no. QC2013C006), and the National Natural Science Foundation of China (Grants nos. 11404055 and 11374353).

References

[1] A. R. Murphy and J. M. J. Fréchet, "Organic semiconducting oligomers for use in thin film transistors," *Chemical Reviews*, vol. 107, no. 4, pp. 1066–1096, 2007.

[2] S. Beaupré, J. Dumas, and M. Leclerc, "Toward the development of new textile/plastic electrochromic cells using triphenylamine-based copolymers," *Chemistry of Materials*, vol. 18, no. 17, pp. 4011–4018, 2006.

[3] Y.-J. Cheng, S.-H. Yang, and C.-S. Hsu, "Synthesis of conjugated polymers for organic solar cell applications," *Chemical Reviews*, vol. 109, no. 11, pp. 5868–5923, 2009.

[4] X. F. Liu, Y. M. Sun, B. B. Y. Hsu et al., "Design and properties of intermediate-sized narrow band-gap conjugated molecules relevant to solution-processed organic solar cells," *Journal of the American Chemical Society*, vol. 136, no. 15, pp. 5697–5708, 2014.

[5] H. Meier, "Conjugated oligomers with terminal donor-acceptor substitution," *Angewandte Chemie—International Edition*, vol. 44, no. 17, pp. 2482–2506, 2005.

[6] D. M. Guldi and M. Prato, "Excited-state properties of C60 fullerene derivatives," *Accounts of Chemical Research*, vol. 33, no. 10, pp. 695–703, 2000.

[7] Z. He, C. Zhong, X. Huang et al., "Simultaneous enhancement of open-circuit voltage, short-circuit current density, and fill factor in polymer solar cells," *Advanced Materials*, vol. 23, no. 40, pp. 4636–4643, 2011.

[8] H.-S. Kim, C.-R. Lee, J.-H. Im et al., "Lead iodide perovskite sensitized all-solid-state submicron thin film mesoscopic solar cell with efficiency exceeding 9%," *Scientific Reports*, vol. 2, article 591, 2012.

[9] J. You, C.-C. Chen, Z. Hong et al., "10.2% power conversion efficiency polymer tandem solar cells consisting of two identical sub-cells," *Advanced Materials*, vol. 25, no. 29, pp. 3973–3978, 2013.

[10] J. A. Love, I. Nagao, Y. Huang et al., "Silaindacenodithiophene-based molecular donor: morphological features and use in the fabrication of compositionally tolerant, high-efficiency bulk heterojunction solar cells," *Journal of the American Chemical Society*, vol. 136, no. 9, pp. 3597–3606, 2014.

[11] B. A. Gregg, "Excitonic solar cells," *Journal of Physical Chemistry B*, vol. 107, no. 20, pp. 4688–4698, 2003.

[12] H. Zeng, X. C. Zhu, Y. Y. Liang, and X. G. Guo, "Interfacial layer engineering for performance enhancement in polymer solar cells," *Polymers*, vol. 7, no. 2, pp. 333–372, 2015.

[13] J. W. P. Hsu and M. T. Lloyd, "Organic/inorganic hybrids for solar energy generation," *MRS Bulletin*, vol. 35, no. 6, pp. 422–428, 2010.

[14] D. Mori, H. Benten, I. Okada, H. Ohkita, and S. Ito, "Low-bandgap donor/acceptor polymer blend solar cells with efficiency exceeding 4%," *Advanced Energy Materials*, vol. 4, no. 3, Article ID 1301006, 2014.

[15] K. C. C. W. S. Klider, F. S. Santos, L. O. Péres, K. Wohnrath, and J. R. Garcia, "Electrochemical synthesis of the copolymer poly(2-methoxy-5-bromo-p-phenylenevinylene)/(2,5-dicyano-p-phenylenevinylene) (MB-PPV/DCN-PPV): tuning properties," *Journal of the Brazilian Chemical Society*, vol. 25, no. 3, pp. 572–578, 2014.

[16] J.-H. Kim, C. E. Song, B. Kim, I.-N. Kang, W. S. Shin, and D.-H. Hwang, "Thieno[3,2-b]thiophene-substituted benzo[1,2-b:4,5-b′]dithiophene as a promising building block for low bandgap semiconducting polymers for high-performance single and tandem organic photovoltaic cells," *Chemistry of Materials*, vol. 26, no. 2, pp. 1234–1242, 2014.

[17] M. Yu, L. Zhang, Q. Peng, H. Zhao, and J. Gao, "Narrow-band gap Benzodipyrrolidone (BDPD) based donor conjugated polymer: a theoretical investigation," *Computational and Theoretical Chemistry*, vol. 1055, pp. 88–93, 2015.

[18] S. Narayanana, S. P. Raghunathana, S. Mathewb et al., "Synthesis and third-order nonlinear optical properties of low band gap 3,4-ethylenedioxythiophene-quinoxaline copolymers," *European Polymer Journal*, vol. 64, pp. 157–169, 2015.

[19] Z. F. Tan, I. Imae, K. Komaguchi, Y. Ooyama, J. Ohshita, and Y. Harima, "Effects of π-conjugated side chains on properties and performances of photovoltaic copolymers," *Synthetic Metals*, vol. 187, no. 1, pp. 30–36, 2014.

[20] P. Hohenberg and W. Kohn, "Inhomogeneous electron gas," *Physical Review*, vol. 136, pp. B864–B871, 1964.

[21] W. Kohn and L. J. Sham, "Quantum density oscillations in an inhomogeneous electron gas," *Physical Review*, vol. 137, no. 6, pp. A1697–A1705, 1965.

[22] A. D. Becke, "Density-functional exchange-energy approximation with correct asymptotic behavior," *Physical Review A*, vol. 38, no. 6, pp. 3098–3100, 1988.

[23] A. D. Becke, "Density-functional thermochemistry. I. The effect of the exchange-only gradient correction," *The Journal of Chemical Physics*, vol. 96, no. 3, p. 2155, 1992.

[24] C. Lee, W. Yang, and R. G. Parr, "Development of the Colle-Salvetti correlation-energy formula into a functional of the electron density," *Physical Review B*, vol. 37, no. 2, pp. 785–789, 1988.

[25] M. J. Frish, G. W. Trucks, H. B. Schlegel et al., *Gaussian 09, Revision A.02*, Gaussian, Waiilingford, Conn, USA, 2009.

[26] M. Sun and H. Xu, "Direct visualization of the chemical mechanism in SERRS of 4-aminothiophenol/metal complexes and metal/4-aminothiophenol/metal junctions," *ChemPhysChem*, vol. 10, no. 2, pp. 392–399, 2009.

[27] Y. Z. Li, T. Pullerits, M. Y. Zhao, and M. T. Sun, "Theoretical characterization of the PC60BM: PDDTT model for an organic solar cell," *Journal of Physical Chemistry C*, vol. 115, no. 44, pp. 21865–21873, 2011.

[28] P. Song, Y. Z. Li, F. C. Ma, T. Pullerits, and M. T. Sun, "External electric field-dependent photoinduced charge transfer in a donor-acceptor system for an organic solar cell," *Journal of Physical Chemistry C*, vol. 117, no. 31, pp. 15879–15889, 2013.

[29] X. M. Zhao and M. D. Chen, "DFT study on the influence of electric field on surface-enhanced Raman scattering from pyridine–metal complex," *Journal of Raman Spectroscopy*, vol. 45, no. 1, pp. 62–67, 2014.

[30] E. K. U. Gross and W. Kohn, "Local density-functional theory of frequency-dependent linear response," *Physical Review Letters*, vol. 55, no. 26, pp. 2850–2852, 1985.

[31] T. Yanai, D. P. Tew, and N. C. Handy, "A new hybrid exchange-correlation functional using the Coulomb-attenuating method (CAM-B3LYP)," *Chemical Physics Letters*, vol. 393, no. 1–3, pp. 51–57, 2004.

[32] M. C. Scharber, D. Mühlbacher, M. Koppe et al., "Design rules for donors in bulk-heterojunction solar cells—towards 10% energy-conversion efficiency," *Advanced Materials*, vol. 18, no. 6, pp. 789–794, 2006.

[33] C.-G. Zhan, J. A. Nichols, and D. A. Dixon, "Ionization potential, electron affinity, electronegativity, hardness, and electron excitation energy: molecular properties from density functional theory orbital energies," *The Journal of Physical Chemistry A*, vol. 107, no. 20, pp. 4184–4195, 2003.

[34] G. Zhang and C. B. Musgrave, "Comparison of DFT methods for molecular orbital eigenvalue calculations," *Journal of Physical Chemistry A*, vol. 111, no. 8, pp. 1554–1561, 2007.

[35] R. A. Marcus, "Electron transfer reaction in chemistry: theory and experment," *Angewandte Chemie International Edition*, vol. 32, pp. 1111–1121, 1993.

[36] R. A. Marcus and N. Sutin, "Electron transfers in chemistry and biology," *Biochimica et Biophysica Acta*, vol. 811, no. 3, pp. 265–322, 1985.

[37] X.-Y. Li, J. Tong, and F.-C. He, "Ab initio calculation for inner reorganization energy of gasphase electron transfer in organic molecule-ion systems," *Chemical Physics*, vol. 260, no. 3, pp. 283–294, 2000.

[38] J. Calvo-Castro, C. J. McHugh, and A. J. McLean, "Torsional angle dependence and switching of inner sphere reorganisation energies for electron and hole transfer processes involving phenyl substituted diketopyrrolopyrroles; a density functional study," *Dyes and Pigments*, vol. 113, pp. 609–617, 2015.

[39] H. Imahori, H. Yamada, D. M. Guldi et al., "Comparison of reorganization energies for intra- and intermolecular electron transfer," *Angewandte Chemie—International Edition*, vol. 41, no. 13, pp. 2344–2347, 2002.

[40] D. P. McMahon and A. Troisi, "Evaluation of the external reorganization energy of polyacenes," *Journal of Physical Chemistry Letters*, vol. 1, no. 6, pp. 941–946, 2010.

[41] J.-L. Brédas, D. Beljonne, V. Coropceanu, and J. Cornil, "Charge-transfer and energy-transfer processes in π-conjugated oligomers and polymers: a molecular picture," *Chemical Reviews*, vol. 104, no. 11, pp. 4971–5003, 2004.

[42] B. A. Gregg, "Interfacial processes in the dye-sensitized solar cell," *Coordination Chemistry Reviews*, vol. 248, no. 13-14, pp. 1215–1224, 2004.